

# Can retired galaxies mimic active galaxies? Clues from the Sloan Digital Sky Survey

G. Stasińska<sup>1</sup>, N. V. Asari<sup>2,1</sup>, R. Cid Fernandes<sup>2,1</sup>, J. M. Gomes<sup>2,1</sup>,  
M. Schlickmann<sup>2</sup>, A. Mateus<sup>3</sup>, W. Schoenell<sup>2,4</sup>, L. Sodr e Jr.<sup>4</sup>  
(the SEAGal collaboration)\*

<sup>1</sup>LUTH, Observatoire de Paris, CNRS, Universit  Paris Diderot; Place Jules Janssen 92190 Meudon, France

<sup>2</sup>Depto. de F sica - CFM - Universidade Federal de Santa Catarina, Florian polis, SC, Brazil

<sup>3</sup>Laboratoire d'Astrophysique de Marseille, CNRS UMR6110, Traverse du Siphon, 13012 Marseille, France

<sup>4</sup>Instituto de Astronomia, Geof sica e Ci ncias Atmosf ricas, Universidade de S o Paulo, S o Paulo, SP, Brazil

8 November 2021

## ABSTRACT

The classification of galaxies as star forming or active is generally done in the ([O III]/H $\beta$ , [N II]/H $\alpha$ ) plane. The Sloan Digital Sky Survey (SDSS) has revealed that, in this plane, the distribution of galaxies looks like the two wings of a seagull. Galaxies in the right wing are referred to as Seyfert/LINERs, leading to the idea that non-stellar activity in galaxies is a very common phenomenon. Here, we argue that a large fraction of the systems in the right wing could actually be galaxies which stopped forming stars. The ionization in these “retired” galaxies would be produced by hot post-AGB stars and white dwarfs. Our argumentation is based on a stellar population analysis of the galaxies via our STARLIGHT code and on photoionization models using the Lyman continuum radiation predicted for this population. The proportion of LINER galaxies that can be explained in such a way is however uncertain. We further show how observational selection effects account for the shape of the right wing. Our study suggests that nuclear activity may not be as common as thought. If retired galaxies do explain a large part of the seagull’s right wing, some of the work concerning nuclear activity in galaxies, as inferred from SDSS data, will have to be revised.

**Key words:** Galaxies: general -Galaxies: active - Stars: AGB and post-AGB

## 1 INTRODUCTION

In the Baldwin, Phillips & Terlevich (1981, BPT) diagram which is used to isolate star forming from active galaxies, the galaxies from the Sloan Digital Sky Survey (SDSS; York et al. 2000) occupy a well-defined region, evoking the wings of a flying seagull. The left wing consists of star forming (SF) galaxies while the right wing is attributed to galaxies with an active nucleus (Kauffmann et al. 2003, Stasińska et al. 2006). The right wing has been subdivided into an upper and a lower branch, called “Seyfert” and “LINER” branch respectively (Kewley et al. 2006). This denomination is given with reference to the typical emission line ratios of active galactic *nuclei* (LINER stands for “Low Ionization Nuclear Emission Regions” in the original paper by Heckman 1980). However, it is by no means obvious that all galaxies of the right wing are powered by an energetically-dominant active nucleus, i.e., that they are genuine Seyferts or LINERs. Binette et al. (1994) found that, in early-type galaxies that have stopped forming stars, hot post-AGB

stars and white dwarfs provide enough ionizing photons to account for the observed H $\alpha$  equivalent widths and can explain the LINER-like emission line ratios observed in such galaxies (see also Sodr e & Stasińska 1999). Taniguchi et al. (2000) followed up this idea, proposing that some LINERs could be post starburst nuclei powered by planetary nebulae central stars.

In Binette et al. (1994), the comparison with observations was very limited, due to the scarcity of adequate data at that time. With the SDSS, we have a homogeneous data base of over half a million galaxy spectra. In addition, the techniques to extract emission lines after modelling the stellar continuum using population synthesis (Kauffmann et al. 2003, Cid Fernandes et al. 2005) now allow emission line measurement even in objects where these lines are difficult to detect in the raw spectra.

The computations by Binette et al. (1994) and Taniguchi et al. (2000) were based on *ab initio* stellar population models. Here, we *directly* use the populations inferred from detailed fits of the observed galaxy spectra to compute the Lyman continuum radiation and estimate its impact on the emission lines. The radiation from the post-AGB and white dwarf stars present in old stellar popula-

\* Semi-Empirical Analysis of Galaxies

tions is much harder than the one from young stars, so that galaxies that are not forming stars presently will contain hotter emission-line regions, and lie *above* the pure star-forming sequence in the BPT diagram. In the remaining of this letter we qualify these galaxies as *retired*<sup>1</sup>.

We explore the expected properties of retired galaxies in terms of their line luminosities and their location in emission line diagnostic diagrams.

## 2 DATA BASE

### 2.1 Sample and data processing

This work analyses data extracted from SDSS Data Release 5 (Adelman-McCarthy et al. 2007). Our parent sample is defined as the 573141 objects spectroscopically classified as galaxies and with no duplicates. We also adopt the following criteria:  $14.5 \leq m_r \leq 17.77$  (from the definition of the Main Galaxy Sample), a minimum  $S/N$  of 10 at  $\sim 4750 \text{ \AA}$  (to ensure a reliable stellar population analysis),  $z \geq 0.002$  (to avoid intragalactic sources) and total z-band light inside the fiber  $> 20\%$  (to reduce aperture effects).

The data are processed as in Cid Fernandes et al. (2005) and Mateus et al. (2006). The stellar populations composing a galaxy are inferred through a pixel-by-pixel modelling of its continuum with our code STARLIGHT, using a base of simple stellar populations computed with the evolutionary population synthesis code of Bruzual & Charlot (2003, BC03). The emission lines are then measured by fitting gaussians to the residual spectrum. We use the same base of 150 stellar populations with ages  $1 \text{ Myr} < t_* < 18 \text{ Gyr}$ , and metallicities  $0.005 < Z_*/Z_\odot < 2.5$  as Cid Fernandes et al. (2007). Illustrative fits are presented in Asari et al. (2007).

### 2.2 Chopping the seagull

Given the distribution of the galaxies in the BPT plane ( $[\text{O III}]/\text{H}\beta$  vs  $[\text{N II}]/\text{H}\alpha$ ), it is convenient to use polar coordinates ( $r, \theta$ ), with the centre defined at the point of inflection of the median curve for the distribution of  $[\text{O III}]/\text{H}\beta$  as a function of  $[\text{N II}]/\text{H}\alpha$ : ( $\log [\text{N II}]/\text{H}\alpha = -0.43$ ;  $\log [\text{O III}]/\text{H}\beta = -0.49$ ). The SF wing corresponds to  $\theta \sim 117^\circ$  for the low-metallicity branch, and  $\sim -94^\circ$  for the high-metallicity branch, while the right wing corresponds to  $\theta = 45-90^\circ$ , with  $\theta \sim 77^\circ$  for Seyferts and  $\sim 59^\circ$  for LINERs. Emission line properties, stellar populations and the corresponding ionizing spectra were obtained after chopping the seagull in 40 angular and 18 radial bins, as shown in Fig. 1, and analysed for different bins in  $\theta$ , as a function of the radial bin index,  $i_r$ .

## 3 THE STARS IN THE SEAGULL'S WINGS

### 3.1 Two extreme cases to consider

Two versions of the ionizing spectrum are considered for each bin: One including all the stellar populations inferred from the synthesis (case F, for “full”) and another with the contribution of populations younger than  $10^{7.5}$  yr set to zero (case O, for “old”). The reason is

<sup>1</sup> *Retired* is to be opposed to *active*, with reference to star formation. We avoid using the term *passive* since this might suggest “without emission lines” (Miller et al., 2003). Ironically, as shown in this letter, a fraction of so-called *active galaxies*, by reference to *nuclear activity* (e.g. Kauffmann & Heckman 2005), could be genuine *retired galaxies*.

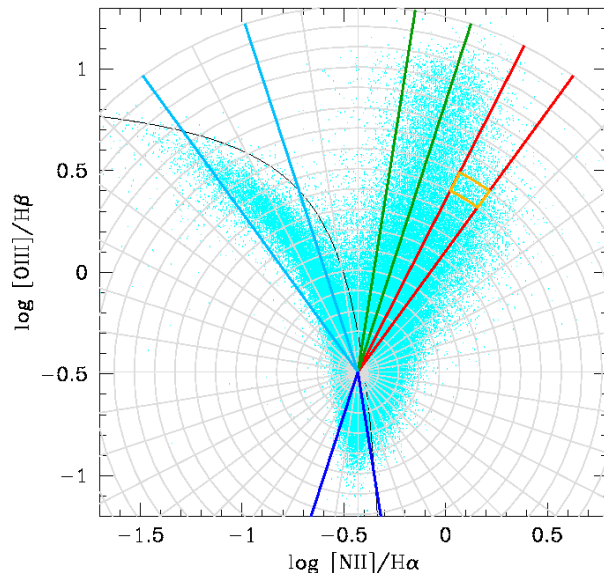


**Figure 1.** The chopped seagull and the definition of the SF branches (light blue and dark blue), Seyfert branch (green) and LINER branch (red). The data points represent all the galaxies defined in Sect. 2.1 that have  $S/N > 3$  in the 4 lines involved in the plot (131287 objects). The black curve is the upper envelope of pure SF galaxies according to Stasińska et al. (2006).

that, due to errors in the data and uncertainties inherent to population synthesis, spectral fits of galaxies without current star formation may attribute a small amount of light to young populations.

For instance, along the LINER branch for  $i_r > 7$ , we obtain light fractions  $x_Y$  of  $\sim 1\%$  at  $4020 \text{ \AA}$  for populations younger than  $10^{7.5}$  yr. This corresponds to mass fractions of less than  $10^{-5}$  and is clearly noise. Yet, given the 5 orders of magnitude difference between ionizing fluxes of young and old populations, even such optically insignificant fractions can have a substantial impact on the shape and intensity of the radiation field in the Lyman continuum of hydrogen. Setting  $x_Y = 0$  circumvents this problem, while at the same time emphasizing the effects of post-AGB stars alone.

Along the Seyfert branch, on the other hand,  $x_Y$  averages to 7%, implying that Seyferts have younger stars than LINERs, in full agreement with both SDSS (e.g., Kauffmann et al. 2003) and independent studies (e.g., González Delgado et al. 2004). All this is clearly illustrated in Fig. 3 of Cid Fernandes et al. (2008), where we show how star-formation histories vary across the BPT diagram.

We now ask: what is the impact of the ionizing radiation produced by the stars responsible for the optical continuum upon the emission lines in galaxies?

### 3.2 The number of ionizing photons

The first question to examine is whether the ionizing photons from the evolved stellar populations are enough to account for the observed  $\text{H}\alpha$  luminosities in the seagull’s wings. For each galaxy, we compute  $Q_{\text{HI}}$ , the number of stellar photons with energies above 13.6 eV arising from the populations uncovered with STARLIGHT (we use the BC03 models also in the Lyman continuum). We then estimate  $L(\text{H}\alpha)_{\text{exp}}$ , the  $\text{H}\alpha$  luminosity expected if all these ionizing photons are absorbed by the gas present in the galaxies, and compare it to  $L(\text{H}\alpha)_{\text{obs}}$ , the observed value corrected for extinction using  $\text{H}\alpha/\text{H}\beta$  and the Cardelli et al. (1989) extinction law for  $R_V=3.1$ . In each bin of the chopped seagull, we define the median

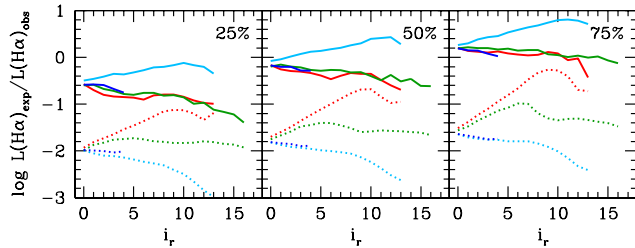


**Figure 2.** Variations of  $L(\text{H}\alpha)_{\text{exp}}/L(\text{H}\alpha)_{\text{obs}}$  along  $i_r$  for the upper SF branch (light blue), lower SF branch (dark blue), Seyfert branch (green) and LINER branch (red). Full lines: case F; dotted lines: case O. The middle panel shows the median value of  $L(\text{H}\alpha)_{\text{exp}}/L(\text{H}\alpha)_{\text{obs}}$ , while the left and right ones show the 25 and 75 quartiles.

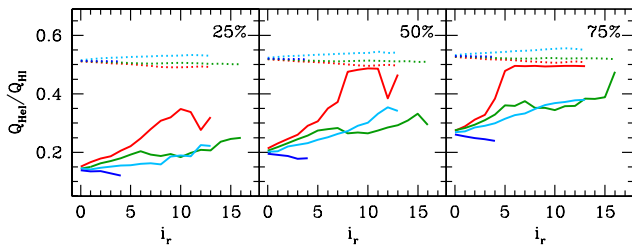


**Figure 3.** Variation of  $Q_{\text{HeI}}/Q_{\text{HI}}$  along  $i_r$ . Conventions as in Fig. 2.

and quartiles of the  $L(\text{H}\alpha)_{\text{exp}}/L(\text{H}\alpha)_{\text{obs}}$  distributions. In Fig. 2, we plot their values as a function of  $i_r$ , with style and colour coding as indicated in the caption.

We see that, in the LINER branch at large radii, the old stellar populations contribute to the ionizing radiation at least as much as the young ones. Given that  $x_Y$  is very small and thus very uncertain (see Sect. 3.1), old populations could even be dominant. For the Seyfert branch, on the other hand, it is the young stars which provide most of the stellar ionizing photons. For the SF branches, the old populations play no role at all. The dispersion in  $L(\text{H}\alpha)_{\text{exp}}/L(\text{H}\alpha)_{\text{obs}}$  as function of  $i_r$  can be judged by comparing the curves corresponding to the quartiles (left and right panels of Fig. 2) with those corresponding to the median (central panel).

Overall, as seen in Fig. 2, while the stellar populations corresponding to case F can largely explain the upper star-forming branch in terms of total number of ionizing photons, they explain only  $\sim 25\%$  of the Seyfert and LINER branches. The central panel of Fig. 2 shows a deficit by a factor 1.5 to 4 for median values of  $L(\text{H}\alpha)_{\text{exp}}/L(\text{H}\alpha)_{\text{obs}}$ . In addition, as mentioned in 3.1, the young stellar populations uncovered by STARLIGHT for the LINER branch are not reliable and case O models could be more appropriate, further increasing the discrepancy. However, our plots are plagued with many uncertainties, as will be discussed in Sect. 5.

### 3.3 The hardness of the ionizing radiation field

The hardness of the ionizing radiation field can be judged by comparing the values of  $Q_{\text{HeI}}$  and  $Q_{\text{HeII}}$  (the number of photons above 24.6 eV and 54.4 eV, respectively), to  $Q_{\text{HI}}$ . Figure 3 shows  $Q_{\text{HeI}}/Q_{\text{HI}}$  as a function of  $i_r$  for the same values of  $\theta$  as in Fig. 2. Again, we show curves for galaxies whose  $Q_{\text{HeI}}/Q_{\text{HI}}$  values correspond to the quartiles (left and right panels) and the median

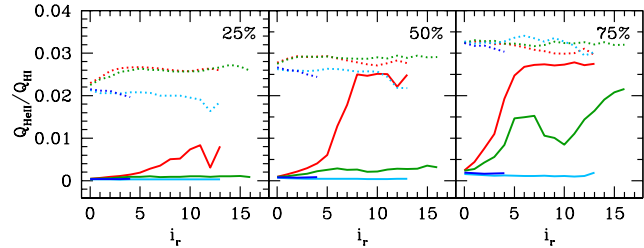


**Figure 4.** Variation of  $Q_{\text{HeII}}/Q_{\text{HI}}$  along  $i_r$ . Conventions as in Fig. 2.

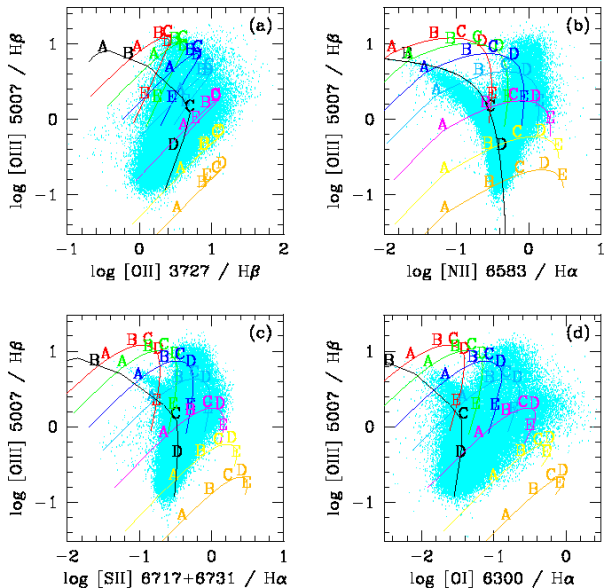
(central panel) of the distribution of  $Q_{\text{HeI}}/Q_{\text{HI}}$  for each branch. It is clearly seen that the radiation produced by the stellar populations in the LINER branch is much harder than in the SF and Seyfert branches, especially for  $i_r > 5$ . Note also that the curves for Seyfert and upper SF branches are similar. This is likely the result of a “cosmic conspiracy”. While, for the SF branch, the hardening of the radiation is due to the decrease of metallicity (McGaugh 1991), the origin of the hardening in the Seyfert branch stems from an increasing population of old stars (see Fig. 3 of Cid Fernandes et al. 2008). As expected, the curves for case O indicate harder radiation, and reach a maximum equal to the typical value corresponding to evolved stellar populations containing hot post-AGB stars and white dwarfs.

Fig. 4 is analogous to Fig. 3 for  $Q_{\text{HeII}}/Q_{\text{HI}}$  and shows a very different behaviour of the LINER branch with respect to the other branches, since the effect of hot post-AGB stars and white dwarfs is here dominant. Note that the values of  $Q_{\text{HeII}}$  do not take into account the X-ray radiation produced by hot stars as well as by X-ray binaries, both of which could have a non-negligible contribution to  $Q_{\text{HeII}}/Q_{\text{HI}}$ .

## 4 PHOTOIONIZATION MODELS FOR THE RIGHT WING

In photoionized nebulae, the emission line ratios are basically determined by three parameters: the hardness of the ionizing radiation, the nebular metallicity and the ionization parameter  $U$  (defined as  $Q_{\text{HI}}/(4\pi R^2 n c)$  where  $R$  is nebular radius,  $n$  is the gas density and  $c$  is the speed of light). We present photoionization models using the ionizing radiation from the stellar populations corresponding to Figs. 3 and 4 for case F. Not much is known about the gas distribution in the galaxies of the right wing. For simplicity, we have assumed a thin shell geometry, with density  $n = 500 \text{ cm}^{-3}$ . Using the code PHOTO, we have computed models with different values of  $U$  and of the nebular metallicity  $Z$  (defined as the oxygen abundance in units of  $4.9 \times 10^{-4}$ , the solar value from Allende Prieto et al. 2001). The abundances of the other elements follow the same prescriptions as in Stasińska et al. (2006).

We first discuss the LINER branch. In Fig. 5, we show the location of several model sequences in classical line ratio diagrams, superimposed on the data points. Each sequence has  $Z$  varying from 0.03 to  $6 Z_{\odot}$ , and is defined by  $U$  as indicated in the figure caption. The ionizing radiation for all the models is given by the stellar population of the galaxy having the median value of  $Q_{\text{HeI}}/Q_{\text{HI}}$  in the bin marked in orange in Fig. 1. Note that the results are almost the same when changing the radiation field from  $i_r=7$  upwards in the LINER branch. We see in Fig. 5 that models with metallicities twice solar cover the tip of the LINER branch in



**Figure 5.** Our sample galaxies in four classical emission line ratio diagrams:  $[\text{O III}]/\text{H}\beta$  versus:  $[\text{O II}]/\text{H}\beta$  (a),  $[\text{N II}]/\text{H}\alpha$  (b),  $[\text{S II}]/\text{H}\alpha$  (c) and  $[\text{O I}]/\text{H}\beta$  (d). Model sequences for the LINER branch are shown for different values of  $\log U$ : -2.3 (red), -2.7 (green), -3 (blue), -3.3 (cyan), -3.7 (purple), -4 (yellow), -4.4 (orange). The black line is the model sequence for SF galaxies from Stasińska et al. (2006). The metallicities  $Z/Z_{\odot}$  are marked with letters as follows: 0.2 (A), 0.5 (B), 1 (C), 2 (D), 5 (E).

the BPT diagram, provided that  $\log U$  is between -3 and -4. Models with even higher  $Z$  can be found in this same region. With the softer radiation field corresponding to smaller values of  $i_r$ , one produces models that can cover the inner part of the LINER branch. We conclude that the radiation from old stellar population in metal rich galaxies can easily account for the emission line ratios observed in the LINER branch. The other diagrams shown in Fig. 5 are also in reasonable agreement with this proposition.

We now turn to the Seyfert branch. Here, the ionizing radiation field provided by the evolved stellar populations is significantly softer than in the LINER branch, as seen from Figs. 3 and 4. Therefore, one can infer from Fig. 5 that the emission line ratios for the upper Seyfert branch cannot be explained by stellar radiation alone.

## 5 UNCERTAINTIES

As has just been shown, our models indicate that the old stellar populations responsible for the optical continua of the considered galaxies can explain the observed emission line ratios of the LINER branch. However the observed  $\text{H}\alpha$  luminosities are more difficult to explain. Our case O models reproduce  $L(\text{H}\alpha)_{\text{obs}}$  within a factor 2 for about 25% of the LINER galaxies with  $i_r > 7^2$ . Does this mean that about one quarter of the LINER galaxies are ionized by hot post-AGB and white dwarf stars, the rest being powered by some other source? In view of the many uncertainties involved in this study, such a conclusion would be premature.

First, there are already uncertainties in the mere process of population synthesis fitting of galaxy spectra (see Cid Fernandes

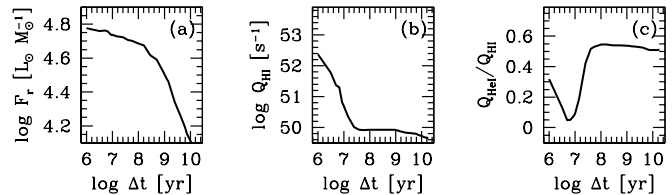


**Figure 6.** Evolution of (a) the  $r$ -band flux, (b)  $Q_{\text{HI}}$  and (c)  $Q_{\text{HeI}}/Q_{\text{HI}}$  for the galaxy corresponding to the median of stellar age in bin  $i_r = 8$  of the upper SF branch.

et al. 2005). Second, the applied extinction correction may not be appropriate.

Perhaps the most important point is that the modelling of the Lyman continuum in old stellar populations is very uncertain. Unfortunately, ready-to-use evolutionary population synthesis codes that compute the ionizing radiation from hot post-AGB and white dwarf stars are scarce. We made experiments with the BC03 code and with PEGASE (Fioc et al. 1997). With BC03, for an instantaneous starburst, we find that  $Q_{\text{HI}}$  depends on the metallicity: it increases by about 0.3 dex from  $Z = Z_{\odot}$  to  $0.02 Z_{\odot}$  at ages larger than  $10^8$  yr, and by over one order of magnitude at around  $10^8$  yr. Therefore, any mistakenly assigned metallicity during the continuum fitting process will induce some error on  $Q_{\text{HI}}$ . With PEGASE, the values of  $Q_{\text{HI}}$  for solar metallicity are larger by 0.2–1 dex than with BC03. What is the reason for such a difference? Different physical ingredients (stellar evolutionary tracks and atmospheres)? Or inaccuracies in the numerical treatments? It seems to us that the major effect comes from the initial-final mass relation of white dwarfs. The analytic form of this relation has been revised recently (Catalán et al 2008), which will certainly lead to changes in the  $Q_{\text{HI}}$  predictions. However, the observational dispersion is very large (see their Fig. 2), so that the predictions will remain uncertain until one understands better the drivers of the initial-final mass relation(s).

## 6 WHY WE SEE A SEAGULL IN THE BPT DIAGRAM

By merging the results of Sects. 3 & 4 with those of Stasińska et al. (2006), we find that photoionization models built with realistic stellar populations are able to cover nearly the entire BPT plane. We now discuss why some regions are avoided by real galaxies.

SF galaxies form a narrow wing because, as shown by Dopita et al. (2006), in regions of star formation the metallicity controls both the ionizing radiation field and the ionization parameter.

But why is the right wing also narrow? Our models for retired galaxies cover the entire space between the two wings of the seagull as well as below the wings. One factor which plays a role in shaping the seagull is that, in order to appear in the BPT diagram, galaxies must be sufficiently bright in the  $r$  band to satisfy the SDSS selection criteria for spectroscopy, and must have the 4 involved emission lines measured with sufficient  $S/N$ . As a matter of fact, the lower border of the right wing is traced by the galaxies with the lowest  $[\text{O III}]$  equivalent widths in our sample.

Metal poor retired galaxies (models A and B in Fig. 5) should be found below the SF wing and between the wings, if they exist and can be detected. As shown in Cid Fernandes et al. (2007), low metallicity SF galaxies are forming stars efficiently (the “downsizing” phenomenon), so that our retired low  $Z$  galaxies (models A and B in Fig. 5) may just be “ahead of their time”. Even if such

<sup>2</sup> For  $i_r < 7$ , the contribution of young stellar populations found by STARLIGHT is likely real, and  $L(\text{H}\alpha)_{\text{obs}}$  is easily reproduced by case F.

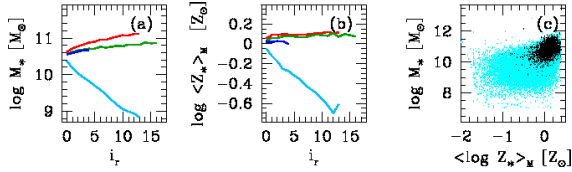


**Figure 7.** The stellar mass  $M_*$  (a) and mean stellar metallicity  $Z_*$  (b) along  $i_r$ , same conventions as Fig. 2. (c)  $M_*$  vs.  $Z_*$ ; cyan: SF galaxies from the BPT diagram, black: galaxies with no [O III] and  $\log [\text{N II}]/\text{H}\alpha < -0.3$ .

galaxies existed, they would be faint both in their emission lines and stellar continuum. To illustrate this, we predict the future evolution of typical low metallicity SF galaxies under the assumption that they stop forming stars now. Applying the models of BC03 to their present-day stellar populations, we find that 0.1 Gyr from now their radiative output will have dropped by a factor of  $\sim 300$ – $1000$  at  $h\nu > 13.6$  eV, and in 1 Gyr their  $r$ -band flux will have faded by  $\sim 0.4$ – $0.8$  mag (Fig. 6). From the observed  $m_r$  distribution of the metal poor SF galaxies in the SDSS, we estimate that over 90% of them should fade beyond the  $m_r < 17.77$  limit by the time they retire. Hence, metal poor retired galaxies either do not exist yet or are too faint, which eliminates all the models below the left wing and between the two wings in Fig 5.

These considerations imply that detectable retired galaxies must have metallicities of the order of solar or larger, and be massive. As shown in Fig. 7a and b, this is in agreement with the mean stellar metallicities ( $Z_*$ ) and masses ( $M_*$ ) obtained using STARLIGHT for those galaxies.

Finally, why are there no SF galaxies with such high metallicities in the BPT diagram? The first idea that comes to mind is that, because of downsizing, such galaxies have already stopped forming stars. There is another possibility, of different nature: nebular metallicities above  $\sim 3 Z_\odot$  lower the electron temperature so much that  $[\text{O III}]\lambda 5007$  cannot be excited (this does not happen in the right wing, since the harder ionizing radiation field produces more efficient heating and compensates the cooling caused by the large metal abundance). Interestingly, there are emission-line galaxies in the SDSS that could well be SF with metallicities larger than  $2$ – $3 Z_\odot$ , i.e. the ancestors of the most metal-rich retired galaxies: they have  $\log [\text{N II}]/\text{H}\alpha < -0.3$  and no [O III]. In Fig. 7c, we plot these galaxies (in black) in a  $M_*$  vs  $Z_*$  diagram, together with the other SF galaxies (in blue). The black points populate the zone of high  $M_*$  and  $Z_*$ , in agreement with our interpretation. It is their high metal content which excludes these likely ancestors of metal rich retired galaxies from the BPT diagram.

Note that the concept of retired galaxies applies also to galaxies that belong to the red sequence studied by Graves et al. (2007) and have such a weak  $\text{H}\beta$  that they do not appear in the BPT diagram, and  $[\text{N II}]\lambda 6584/\text{H}\alpha$  ratios similar to those of LINER galaxies. As a matter of fact, there is a numerous population of such galaxies in the SDSS (over 40,000 using the selection criteria of Sect. 2.1). The weaker  $\text{H}\alpha$  equivalent widths of these galaxies are easily reproduced by our models for retired galaxies.

## 7 CONCLUSION

We have shown that retired galaxies can account for a good part of the LINER branch in the seagull’s right wing. How much exactly is difficult to say, given the uncertainties. If, as we argue, a significant fraction of the LINER galaxies are in fact retired galaxies

– and not active galaxies as generally claimed – the perception of the local Universe would be drastically changed. Nuclear activity would not be as common as thought, and some of the work based on SDSS data and related to the AGN population will have to be reconsidered.

## ACKNOWLEDGEMENTS

This work was supported by the CAPES-COFECUB program. The STARLIGHT project is supported by the Brazilian agencies CNPq, CAPES and FAPESP. The Sloan Digital Sky Survey is a joint project of The University of Chicago, Fermilab, the Institute for Advanced Study, the Japan Participation Group, the Johns Hopkins University, the Los Alamos National Laboratory, the Max-Planck-Institute for Astronomy, the Max-Planck-Institute for Astrophysics, New Mexico State University, Princeton University, the United States Naval Observatory, and the University of Washington. Funding for the project has been provided by the Alfred P. Sloan Foundation, the Participating Institutions, the National Aeronautics and Space Administration, the National Science Foundation, the U.S. Department of Energy, the Japanese Monbukagakusho, and the Max Planck Society. We thank the referee for insightful comments.

## REFERENCES

- Adelman-McCarthy J. K., et al., 2007, ApJS, 172, 634  
 Allende Prieto C., Lambert D. L., Asplund M., 2001, ApJ, 556, L63  
 Asari N. V., Cid Fernandes R., Stasińska G., Torres-Papaqui J. P., Mateus A., Sodr e L., Schoenell W., Gomes J. M., 2007, MNRAS, 381, 263  
 Baldwin J. A., Phillips M. M., & Terlevich R., 1981, PASP, 93, 5  
 Binette L., Magris C. G., Stasińska G., Bruzual A. G., 1994, A&A, 292, 13  
 Bruzual A. G., 2007, IAUS, 241, 125  
 Bruzual G., Charlot S., 2003, MNRAS, 344, 1000  
 Cardelli J. A., Clayton G. C., Mathis J. S., 1989, ApJ, 345, 245  
 Catal n S., Isern J., Garc a-Berro E., Ribas I., 2008, MNRAS, 701  
 Cid Fernandes R., Mateus A., Sodr e L., Stasińska G., Gomes J. M., 2005, MNRAS, 358, 363  
 Cid Fernandes R., Asari N. V., Sodr e L., Stasińska G., Mateus A., Torres-Papaqui J. P., Schoenell W., 2007, MNRAS, 375, L16  
 Cid Fernandes R., et al., 2008, arXiv, 802, arXiv:0802.0849  
 Dopita M. A., et al., 2006, ApJ, 647, 244  
 Fioc M., Rocca-Volmerange B., 1997, A&A, 326, 950  
 Graves G. J., Faber S. M., Schiavon R. P., Yan R., 2007, ApJ, 671, 243  
 Heckman T. M., 1980, A&A, 87, 152  
 Kauffmann G. et al., 2003, MNRAS, 346, 1055  
 Kauffmann G., Heckman T. M., 2005, RSPTA, 363, 621  
 Kewley L. J., Dopita M. A., Sutherland R. S., Heisler C. A., Trevena J., 2001, ApJ, 556, 121  
 Kewley L. J., Groves B., Kauffmann G., Heckman T., 2006, MNRAS, 372, 961  
 Marigo P., Girardi L., Bressan A., Groenewegen M. A. T., Silva L., Granato G. L., 2007, arXiv:0711.4922  
 Mateus A., Sodr e L., Cid Fernandes R., Stasińska G., Schoenell W., Gomes J. M., 2006, MNRAS, 370, 721  
 McGaugh S. S., 1991, ApJ, 380, 140  
 Miller C. J., Nichol R. C., G mez P. L., Hopkins A. M., Bernardi M., 2003, ApJ, 597, 142  
 Sodr e L., Jr., Stasińska G., 1999, A&A, 345, 391  
 Stasińska G., Cid Fernandes R., Mateus A., Sodr e L., Asari N. V., 2006, MNRAS, 371, 972  
 Taniguchi Y., Shioya Y., Murayama T., 2000, AJ, 120, 1265  
 York D. G., et al., 2000, AJ, 120, 1579